Photoelectrochemical uranium extraction from uranium mine tailings seepage water

Yin Ye [1*], Jian Jin [1], Yanru Liang [1], Zemin Qin [1], Xin Tang [1], Yanyue Feng [2], Miao Lv [3], Shiyu Miao [4], Cui Li [1], Yanlong Chen [1], Fan Chen [1*], Yuheng Wang [1*]

[1] *School of Ecology and Environment, Northwestern Polytechnical University, 710129 Xi'an, P. R. China*

[2] *Department of Chemistry and Chemical Engineering, Chalmers University of Technology, SE-41296 Gothenburg, Sweden*

[3] *State Key Laboratory of Urban Water Resource and Environment, School of Environment, Harbin Institute of Technology, Harbin 150090, China*

[4] *College of Eco-Environmental Engineering, Qinghai University, Xining, 810016, P. R. China*

***Corresponding authors:**

Yin Ye: yeyin01@hotmail.com ; yin.ye@nwpu.edu.cn

Yuheng Wang: yuheng.wang@nwpu.edu.cn

Fan Chen: chenfanhit@163.com

Abstract

Extracting uranium (U) from mine tailings seepage water can compensate the depletion of conventional U resources. However, current photocatalytic methods have intrinsic obstacles, such as the recombination of charge carriers, and the deactivation of catalysts by extracted U. Here we show that, by applying a small bias potential on the photocatalyst to drive spatial charge-carriers separation, the photoelectrochemical (PEC) method enables much faster U extraction and exceptional stability. In synthetic U-bearing water, the PEC U extraction proceeds via single-step one-electron reduction. Hence stable U(V) is produced from aqueous media under ambient conditions for the first time, implying the potential to facilitate future studies on U(V) chemistry. In real seepage water, the PEC method achieves a capacity of 0.67 gU $m^{-3} \cdot h^{-1}$ without further optimization, which is 17 times faster than the photocatalytic method using identical photocatalyst. The PEC U extraction method is therefore of broad research interests.

Keywords

Uranium; Extraction; Mine tailings; Seepage water; Photoelectrochemical

Main

Nuclear power, fueled by uranium (U), is a mature low-carbon energy technology that plays a crucial role in the transition to a sustainable future [1]. Along with the rapidly expanding nuclear power industry, public concerns regarding its sustainability have arisen. One is the environmental impact, as billions tons U mine tailings have been disposed worldwide due to mining and processing of U ores [2]. Untreated, the tailings derive large quantities of U-containing (mg/L level) seepage water [2]. As U is highly hazardous to the biosphere, the seepage water would threaten the eco-system if not properly treated [3,4]. Another concern is the vulnerability of the global U supply. Current U supply relies on terrestrial ores, which have limited availabilities and could hardly meet the future demand [5-8]. Hence, recovering U from the seepage water is highly appealing because it not only compensates the depletion of conventional uranium resources but also reduces the negative environmental impact of U mining.

Photocatalysis (PC) is a plausible approach for U extraction from aqueous media [9]. The core processes of the PC U extraction method are the adsorption and reduction of soluble hexavalent U (U(VI), which is the dominant U species under ambient conditions, into insoluble tetravalent uranium (U(IV)) by conduction band electrons generated within the photocatalyst upon illumination. Currently, most research efforts have focused on developing novel photocatalysts [10,11], but two intrinsic obstacles persist (Figure 1a): the fast recombination of charge carriers upon their formation[12], and the blockage of catalyst active sites by precipitated U [11,13]. Consequently, the efficiency of the PC method is limited, and catalyst regeneration is required, which hinders the long-term continuous operation. Therefore, suppressing the recombination of charge carriers, and spatially separating the uranium deposition sites from photocatalyst active sites are the keys to tackle these challenges.

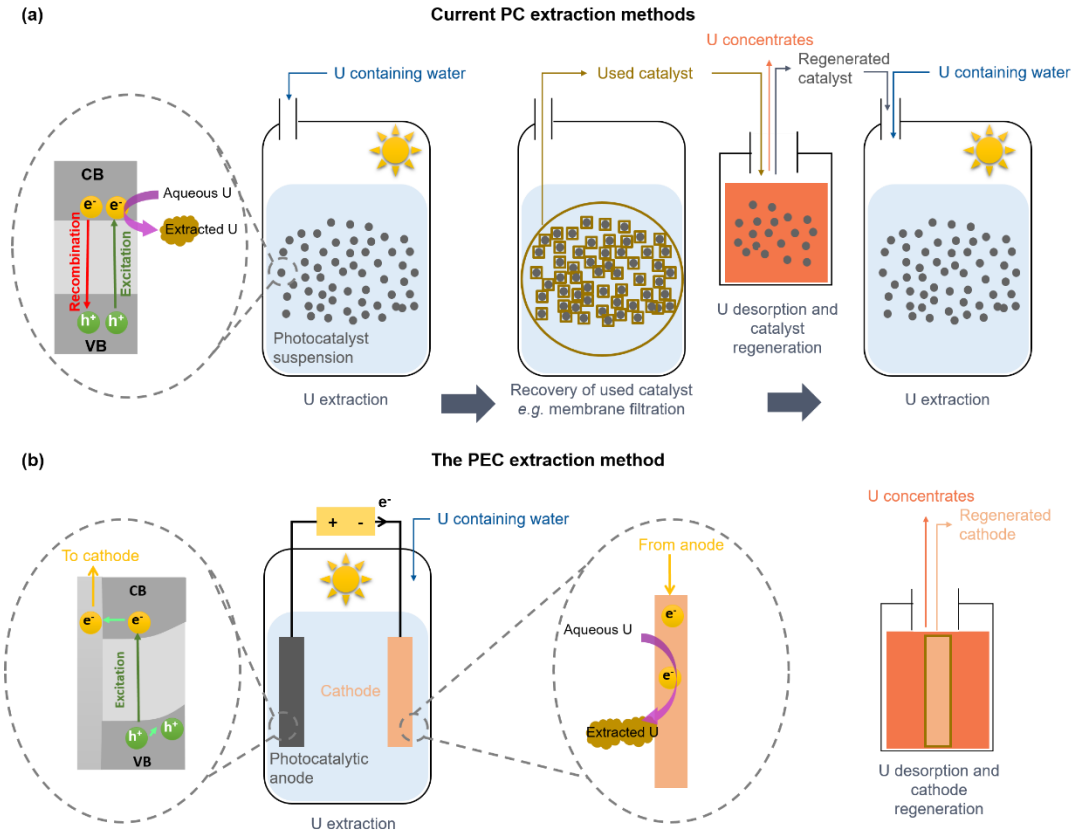

Figure 1. Schematic representations of current PC uranium extraction methods and the proposed PEC uranium extraction method

Here we show that the photoelectrochemical (PEC) method could effectively resolve the aforementioned drawbacks of PC methods, by applying a bias potential on the photocatalyst (Figure 1b). The PEC method enables much faster U extraction and exceptional stability for both synthetic U-containing water and real U mine tailings seepage water. We further show that the bias-driven spatial charge-carriers separation is the key to obtain fast U extraction and high stability. In synthetic U-bearing water, the PEC U extraction proceeds via single-step one-electron reduction. For the first time we produced stable U(V) from aqueous media under ambient conditions without using organic ligands, implying the potential of the PEC method for facile U(V) synthesis, which would significantly facilitate future studies on U(V) chemistry. In real seepage water, the PEC method achieved a capacity of 0.67 gU $m^{-3} \cdot h^{-1}$ without further optimization, which is 17 times faster than the photocatalytic method using identical photocatalyst, at a compulsory energy cost of 125 kWh/kgU ($15.63/kgU). In summary, our work introduces a facile strategy to simultaneously address the depletion of conventional U

resources and the negative environmental impacts of U mining industry, contributing to the sustainability of nuclear power industry.

The PEC U extraction method

We hypothesize that the key to obtaining higher efficiency and stability in PEC uranium extraction is the application of a proper external bias potential on the photocatalyst that can suppress the recombination of charge carriers and spatially separate the U deposition sites from the photocatalyst active sites. To examine this hypothesis, PEC experiments were conducted at varied bias potentials with synthetic U-containing water. Control experiments were also performed with illumination at open-circuit condition (*i.e.*, PC U extraction), and in the dark with external bias (*i.e.*, EC U extraction). Fast PEC U extraction kinetics were obtained at all tested bias potentials, and the total extraction efficiencies after 120 min operation reached 65.2%, 78.7%, and 63.8%, at applied bias potential of 0.0 V (all potentials reported in this work are relative to the standard calomel electrode (SCE) unless otherwise stated), 0.5 V, and 1.0 V respectively (Figure 2a and c). In the case of PC method, U extraction was much slower, where a total efficiency of 28.9% was achieved after 120 min operation. The results implied a significant role of the applied bias in promoting the U extraction efficiency of the PEC method.

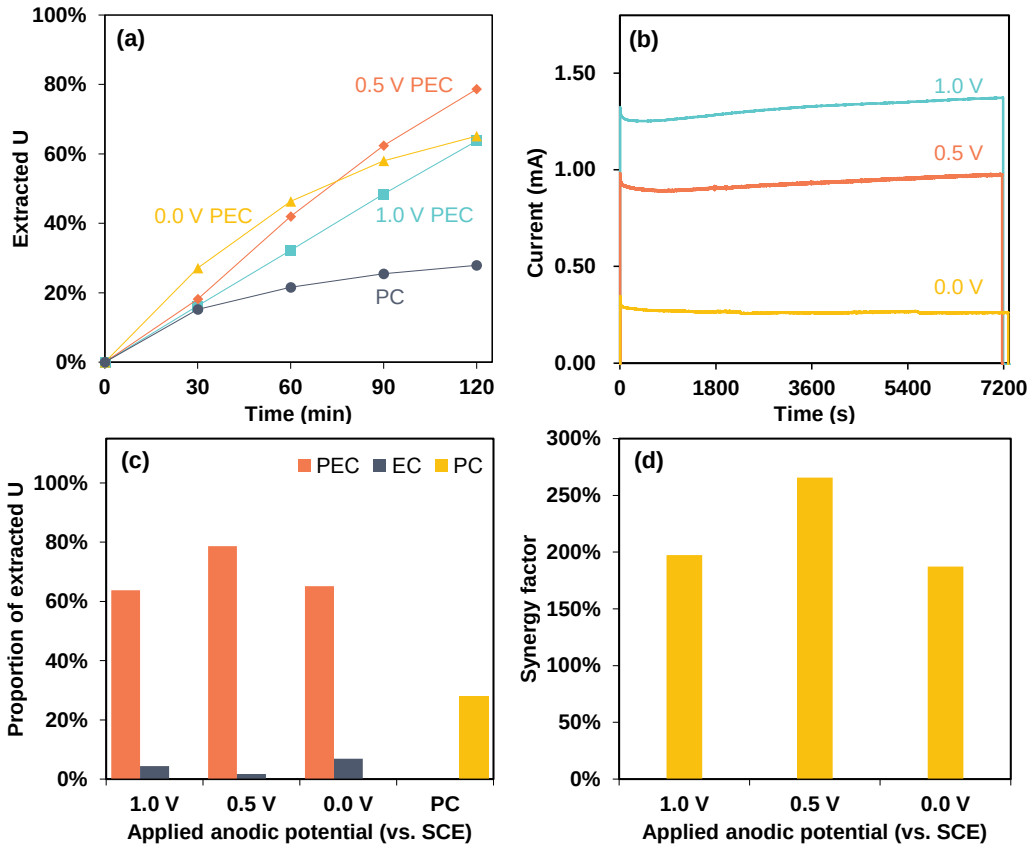

Figure 2. Uranium extraction by PEC and PC methods (a); the current-time plots during PEC U extraction experiments (b); total U extraction efficiencies of different methods after 120 min operation (c); the synergy factors of the PEC method at varied bias potentials (d). Conditions: $[U(VI)]_0$ = 0.05 mM, [NaCl] = 20 mM, natural pH (~4.2).

By comparing the U extraction efficiencies of the EC, PC, and PEC methods, obvious synergistic effects were observed in the PEC method: the synergy factor (calculated according to Supplementary Note 3) at 0.0 V, 0.5 V, and 1.0 V were 187%, 266% and 197%, respectively (Figure 2d). The bias potential might play two roles in PEC U extraction: (1) promoting the separation of charge carriers by triggering band bending within the photocatalyst [14]; (2) driving direct EC U extraction on electrode surfaces [15]. The first role was evidenced by the increased photocurrent with the increasing bias potential (Figure 2b). There was much less EC U extraction at the three bias potentials (≤7%) (Figure 2c and Figure S2), indicating an insignificant contribution of the second role. Furthermore, although the photocurrent increased with higher bias potential, an optimal value exists. This might be attributed to the production of oxidative species at a higher potential that can re-oxidize the precipitated U.

During the PEC U extraction, as the photocurrent (Figure 2b) indicates constant extraction of conduction band electrons from the photocatalyst to the cathode, the U deposition sites and the photocatalyst should be spatially separated, therefore higher stability and durability of the photocatalyst are expected. To test this expectation, we performed a reusability assay (Figure 3a). After each cycle, defined reaction solutions were directly refilled into the PEC reactor and the PC reactor without regeneration treatment of the TiO_2 nanotube array (TNA) and the Ti electrode. The PEC method indeed showed high durability, as ~0.58 mg U could be extracted from 0.06 L synthetic U-containing water for each of the 8 tested 120-min operation cycles. On the contrary, in the first cycle of the PC method, only 0.28 mg U was extracted, and the extracted U decreased to 0.15 mg and 0.10 mg during the second and the third cycle, respectively. Hence, the PEC method had exceptional stability compared to the PC method.

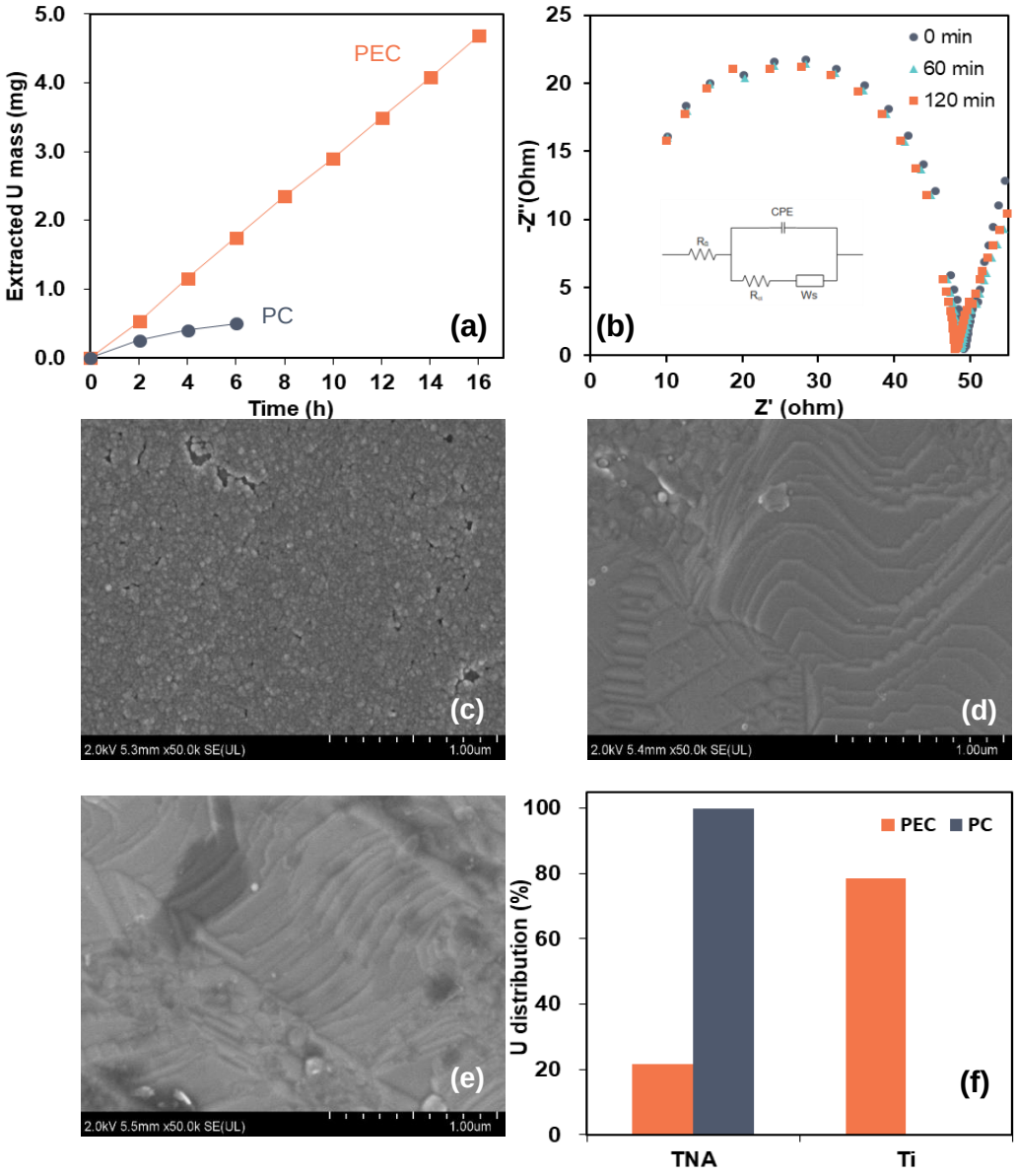

Figure 3. The PEC uranium extraction and the PC uranium extraction during continuous cyclic runs (a); in-situ EIS plots of the Ti electrode during the PEC uranium extraction experiment (b); SEM image of the Ti electrode after PEC uranium extraction (c); SEM image of the Ti electrode after PC uranium extraction (d); SEM image of the fresh Ti electrode (e); comparison of the uranium content on different components after PEC and PC uranium extraction operation (f). Conditions: $[U(VI)]_0$ = 0.05 mM, unadjusted pH (~4.2), [NaCl] = 20 mM, E_{bias} = 0.50 V vs. SCE.

The morphologies of the Ti electrodes upon 120 min PEC and PC U extraction experiments were characterized by scanning electron microscopy (SEM) and compared with that of the fresh

Ti electrode. The results show that, upon PEC treatment, the electrode was covered by a nanoparticles layer (Figure 3c and e), which contains U according to energy dispersive spectroscopy (EDS) analysis (Figure 3f and Figure S4). However, in the case of PC U extraction, no noticeable changes in the electrode morphology (Figure 3d and e) or U deposition (Figure 3f and Figure S5) was observed. We further analyzed the distribution of extracted U on both the TNAs and the Ti electrodes upon PC and PEC experiments (see Supplementary Note 5). The results revealed that, in the case of PC, U extraction products were precipitated exclusively on the TNA photocatalyst (Figure 3f), which confirmed that the blockage of the photocatalyst active sites by extracted U was responsible for the poor stability of the PC U extraction technology [11,13,16]. On the contrary, extracted U was predominantly (78.4%) precipitated on the Ti cathode in the case of PEC (Figure 3f), even though a small fraction was found on the TNA photocatalyst, most probably as adsorbed species [17]. Therefore, the spatial separation of the U precipitation sites and the photocatalyst could explain the stable photoactivity of the TNA photoanode and therefore the stable photoelectrons output in PEC method. More interestingly, the continuously U precipitation onto the Ti cathode in the PEC method did not decrease its U reduction capacity (Figure 3a). To clarify this aspect, in-situ electrochemical impedance spectroscopy (EIS) analysis [18] was carried out to monitor the interfacial charge transfer resistance changes in real-time during the PEC U extraction. The curves shrank slightly during the experiment (Figure 3b), and the fit results revealed gradual decrease in interfacial charge transfer resistance of the Ti cathode (Supplementary Note 6), which could facilitate the U reduction. This finding was consistent with the slightly increasing pattern of the current during one cycle (Figure 2b and Figure S3), and the similar currents among different continuous cycles (Figure S3). The results here suggested that the U precipitates on the Ti cathode could facilitate further U deposition, instead of blocking the active sites.

As the operation conditions may vary greatly among seepage waters from different U mines, the effects of different operation conditions on the performance of the PEC method were examined. We first evaluated the PEC uranium extraction performance at pH from 4.2 to

9.0. The results show that similar U extraction rate in the first 60 min was achieved for all the tested pH values, while lower rate was observed for higher pH at 60-120 min (Figure 4a). One plausible explanation would be the changes in the speciation of aqueous U(VI) with the increasing pH (Figure S7). At acidic pH (4.2), U(VI) was predominantly present as uranyl (UO_2^{2+}) ions, and the complexation of UO_2^{2+} with OH^- or CO_3^{2-} ions increased with the increasing pH. In the case of higher pH, as the U extraction proceeded, the residual aqueous U concentration decreased, so the proportion of UO_2^{2+}-OH^- and UO_2^{2+}-CO_3^{2-} complexes increased with the extraction time. CV curves of the Ti cathode in the synthetic U-containing water at various pH show that these UO_2^{2+}-OH^- and UO_2^{2+}-CO_3^{2-} complexes had more negative reduction potentials than UO_2^{2+} ions (Figure S8), implying that the reduction of these hydroxyl and carbonate complexes predominant at higher pH was less thermodynamically favorable. Moreover, as U reductive precipitation mostly took place on the Ti cathode, the adsorption of U(VI) to the Ti electrode surface should be a prerequisite for its reduction. In the case of higher pH, the electric repulse between the negatively charged UO_2^{2+}-OH^- and UO_2^{2+}-CO_3^{2-} species and the Ti cathode surface might also obstruct the U reduction.

Thereafter, we evaluated the PEC U extraction performance at different initial U concentrations ranging from 0.025 mM to 0.20 mM (Figure 4b and Figure S9). The high initial U concentrations, *i.e.*, 0.10 mM and 0.20 mM, enabled faster kinetics in the first 30 min. As for the low initial U concentrations, *i.e.*, 0.025 mM and 0.05 mM, the accumulation of U precipitates on the Ti cathode, which was beneficial for the extraction of aqueous U, was more difficult [15], so slower initial rates were obtained. But once some U precipitates were deposited, the extraction was accelerated and resulted in similar kinetics with high initial U concentrations in the later phase. In the case of the 0.20 mM U experiment, the extraction rate in the later phase declined and became the slowest, which might be due to the saturation of the active sites [19].

NO_3^- and SO_4^{2-} are abundant in many U mining effluents [20], so their effects on PEC methods were examined. The results show that slightly higher U extraction rates were obtained by replacing the 20 mM NaCl with 20 mM $NaNO_3$ or Na_2SO_4 in the synthetic U-containing

water (Figure 4c). The speciation of aqueous U(VI) could be different in the presence of different anions, because of the different complexation abilities of different anions with U(VI). The electrochemical interactions of these different U(VI) complexes could vary greatly, which was evidenced by CV scans (Figure S10).

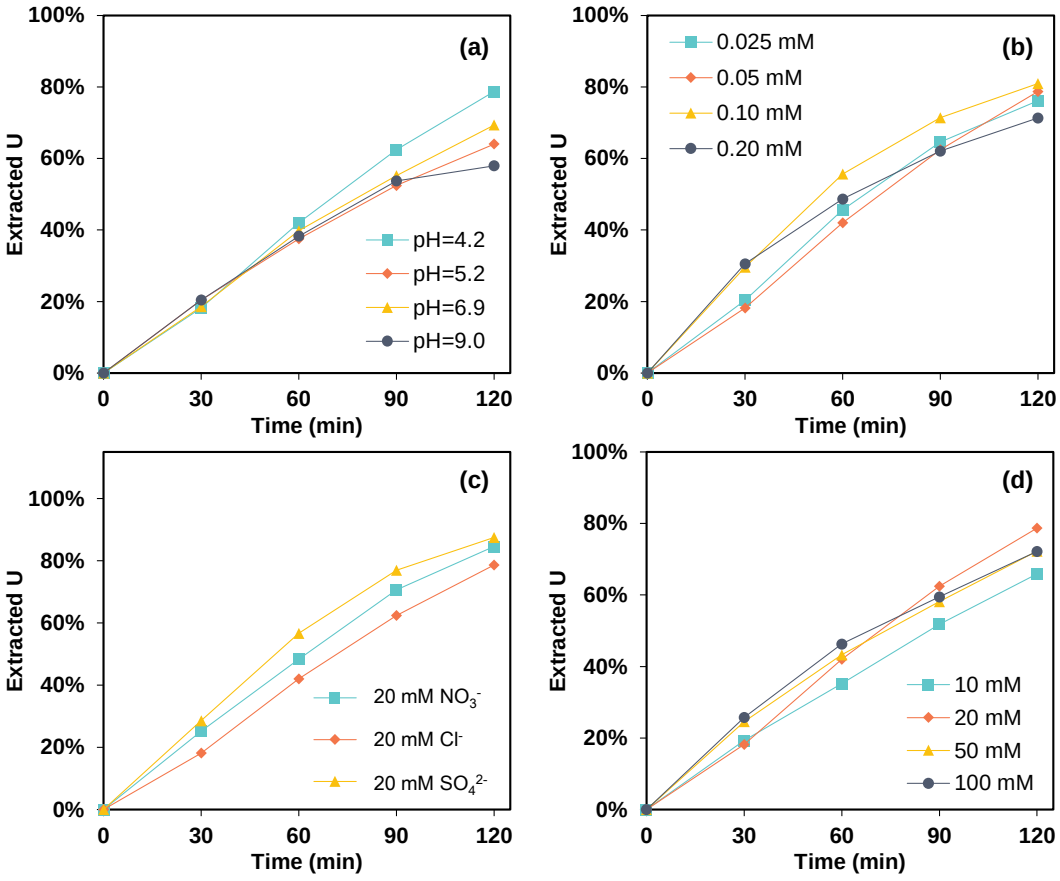

Figure 4. U extraction by PEC at varied pH (a), with varied initial U concentration (b), with the presence of different anions (c), with different electrolyte concentration (d).

The conductivity of the aqueous media, which is correlated to the electrolyte concentration, may affect photoelectrochemical water treatment processes [21]. To examine this aspect, PEC U extraction experiments were conducted at different electrolyte concentrations. The results show that the extraction rate did not vary significantly while the electrolyte (NaCl) concentration increased dramatically from 10 mM to 100 mM (Figure 4d). In typical (photo)electrochemical water treatment systems, the overall charge carriers transfer resistance mainly consists of two components, *i.e.*, the solution/ohmic resistance due to the resistance of the ions transfer in the reaction solution, and the charge transfer barriers at the solution/electrode interfaces [22]. The

currents at varied NaCl concentrations (corresponding to varied conductivity and therefore varied solution/ohmic resistance) were similar (Figure S11), implying that charge transfer barriers at the electrode/solution interfaces dominated the charge transfer resistance in the tested NaCl concentration range.

Mechanisms: formation of stable pentavalent U

To decipher the mechanisms governing the PEC U extraction processes, the electrochemical interactions of aqueous U and the Ti electrode were studied using cyclic voltammetry (CV), and the results are shown in Figure 5a and b. In the presence of U(VI), a reduction peak at around -0.85 V emerged. Meanwhile, an oxidation peak emerged at -0.36 V, in the presence of U(VI). Considering that no redox peaks were detected in the absence of U(VI), all these observed redox peaks can be assigned to the redox changes of U species on the Ti electrode. Further, when increasing scanning rate, the reduction peaks shifted to lower potentials, whereas the oxidation peaks moved to higher potentials (Figure 5b). These reflected the kinetics of the redox reactions [23]. Linear relations between the reduction/reduction peak current values and the square root of scanning rates were identified (Figure S12), suggesting that both the reductive conversion and the oxidative conversion were diffusion-controlled reactions that could be described by the Randles-Sevcik model [23-25]. Fit with the Randles-Sevcik model, the CV data revealed a one-electron U(VI) reduction process on the Ti electrode (see Supplementary Note 8 for details). Therefore, the reduction peaks at around -0.85 V vs. SCE can be assigned to the one-electron reduction of U(VI) to pentavalent U (U(V)) [6,26-28], and the oxidation peaks at -0.36 V vs. SCE represents the oxidation of U(V) to U(VI) [6]. The small variation of the positions of these peaks compared with those in the literature could be attributed to the differences in over potentials of the different applied electrodes and the scan rates. Furthermore, the transferred charges of the oxidation and the reduction peaks were similar (Figure S13), suggesting no significant disproportionation of the U(V) upon its formation on the Ti electrode.

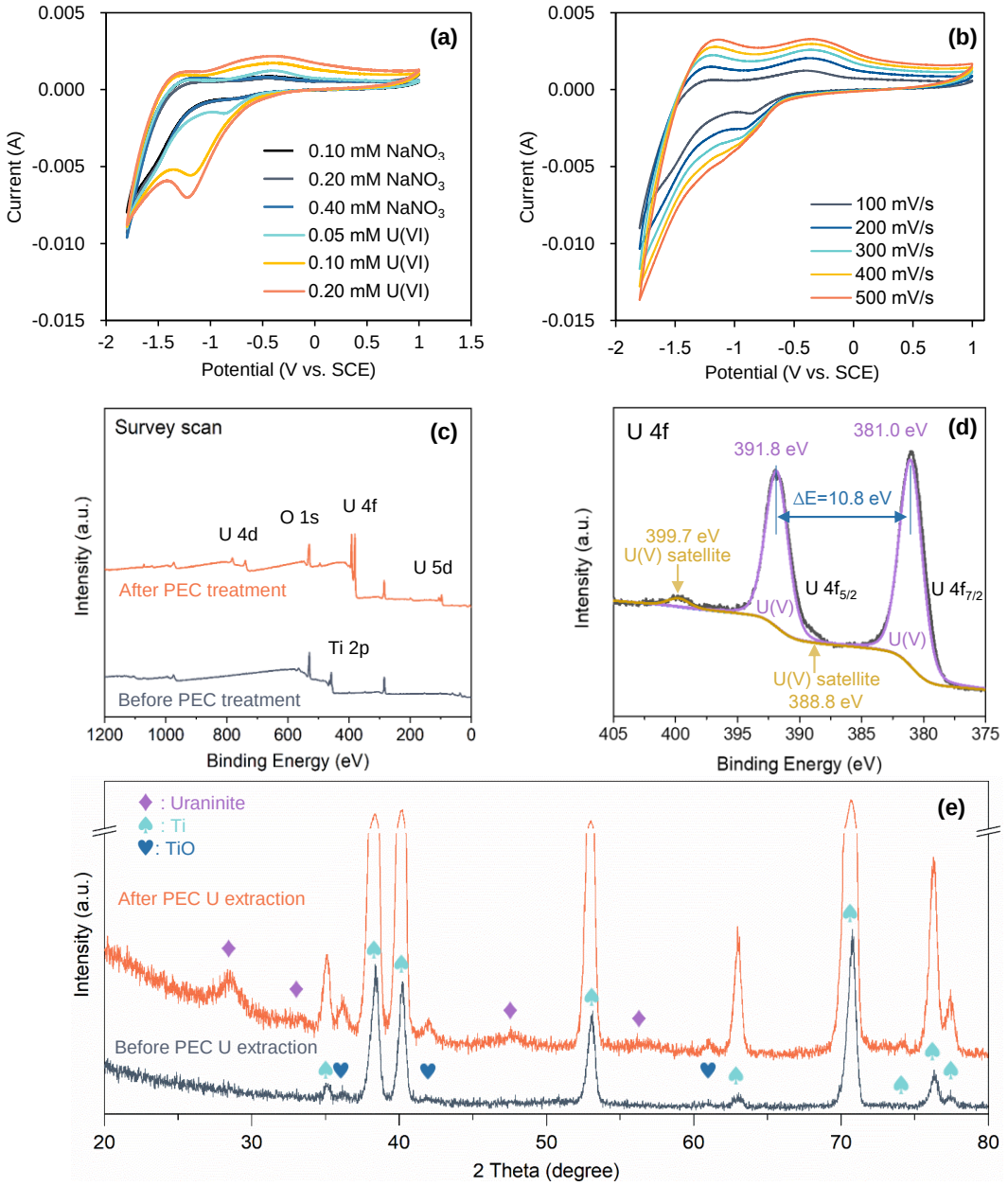

Figure 5. Cyclic voltammograms of the Ti electrode in synthetic water with/without uranium, at a scan rate of 100 mV/s (a), and in synthetic water with 0.05 mM uranium at varied scanning rate (b); XPS survey scan spectra of the Ti electrode before and after PEC uranium extraction (c); XPS U4f scan of the Ti electrode after PEC uranium extraction (d); XRD spectrum of the Ti electrode after PEC uranium extraction (e).

The precipitated U was further characterized to elucidate the PEC U extraction mechanisms. In the X-ray photoelectron spectroscopy (XPS) survey scan spectra, two characteristic U4f peaks emerged after the extraction (Figure 5c), indicating U deposition on

the Ti electrode, consistent with the SEM-EDS results. The mineralogical composition of the PEC extracted U was characterized by X-ray diffraction (XRD). As shown in Figure 5e, upon PEC U extraction, broad Bragg reflection peaks at 2θ = 28.55°, 33.09°, 47.50°, and 56.36° emerged, which could be assigned to uraninite structures. This finding suggests that the PEC extracted U present in the form of uraninite. Although uraninite is nominally UO_2 with a fluorite-type (CaF_2) structure, its actual stoichiometry can vary significantly (UO_{2+x}, $0 \leq x \leq 0.61$) due to the variance of the oxidation state of U [29]. XPS high-resolution U4f scan was then performed to further confirm the oxidation state of the extracted U. The spectrum shows two major peaks separated from each other by ~10.8 eV (Figure 5d). These two peaks could be assigned to the $U4f_{7/2}$ and $U4f_{5/2}$, respectively, and the separation of these two peaks was due to the spin-orbit split [30]. Additionally, two small peaks at 399.7 eV and 388.8 eV were also observed (Figure 5d), which could be assigned to the satellite peaks of U(V) [30,31]. Furthermore, the $U4f_{5/2}$ and $U4f_{7/2}$ peaks were fit [23,31,32], and the results show two strong peaks at 391.8 eV and 381.0 eV, both separated from their corresponding satellite peak by 7.8 eV. Based on these data, the two U4f peaks could both be assigned to U(V) [23,30-34]. The absence of spectral patterns of either U(VI) or U(IV) shows that the PEC extracted U was pentavalent, consistent with the CV characterization. A few studies have shown that U(V) could be stabilized by coordination with iron oxides, carbonate or organic ligands [23,35-39]. However, iron oxides and carbonate were not detected by the XRD analysis, and Fe and organic ligands were absent in the synthetic U-containing water. In comparison, the PC extracted U was a mixture of U(IV) and U(VI) (Figure S15). Hence, one hypothetical explanation could be the stabilization of U(V) in $UO_{2.5}$ uraninite structure on the surface of the Ti electrode, which needs further investigations.

The proposed PEC method opens a new avenue towards the facile synthesis of this often "overlooked" U oxidation state. U(V) chemistry is important for elucidating the biogeochemical behaviors of U in the environment and understanding the properties of the f electrons of actinide ions [40,41]. And a facile U(V) synthesis method is useful for assisting future studies on the U(V) chemistry. Additionally, because of its unique electronic structure [42], stable

U(V) materials is also highly desired for photocatalysis, magnetism, and energy storage applications [42,43]. However, due to fast disproportionation [6], U(V) species are usually very unstable [9,13,19,44]. Attempts have been made by pioneers in synthesizing stable U(V), but the state-of-the-art methods are complicated and time-consuming, requiring the addition of organic ligands, heating, high pressure, and/or high voltage [33,34,41-43,45,46]. To our best knowledge, this study is the first in successfully producing stable U(V) from aqueous media without adding organic ligands, under ambient conditions and in open air. This would significantly facilitate future studies on U(V) chemistry.

Recovery of extracted U from the Ti electrode

The recoverability of the extracted U on Ti electrode was evaluated. Both the physicochemical method and the electrochemical method were examined (see Supplementary Note 9 for details). As shown in Figure S16, by the physicochemical method, the 0.1 M HCl could recover 66.3% of the extracted U. By applying a bias voltage, the elution of the extracted U could be promoted. In the 0.1 M HCl elution solution, the U recovery rate was 83.2% at 1.0 V bias voltage and 100.0% at 1.5 V, respectively. Therefore, the PEC extracted U species on the Ti electrode could be fully recovered by applying a dilute acid and a low bias voltage.

U extraction in real U mine tailings seepage water

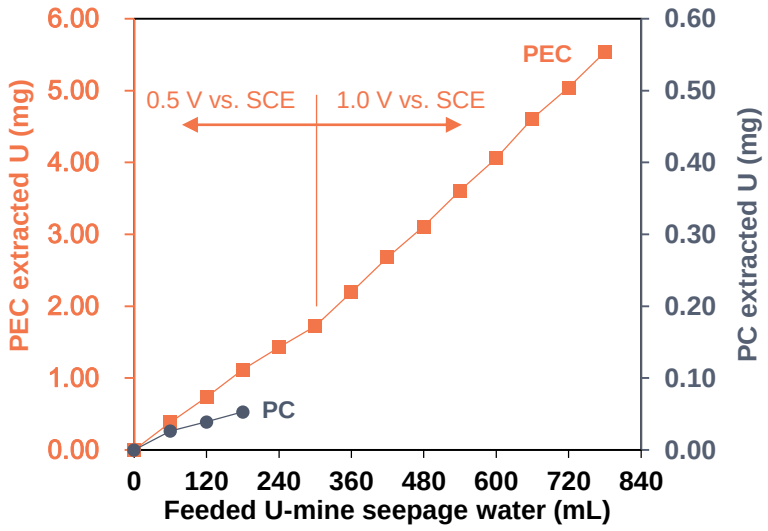

Figure 6. Long-term uranium extraction performances of the PEC method and the PC method during continuous cyclic runs in real uranium-mine tailings seepage water

The U extraction performance of the proposed PEC method in real U-mine seepage water was also evaluated, and the results are present in Figure 6. The U extraction capacity of the PC method was only 0.04 gU $m^{-3}{\cdot}h^{-1}$, and decreased dramatically to 0.02 gU $m^{-3}{\cdot}h^{-1}$ after only 2 cycles. For comparison, the PEC method extracted 5.54 mg U from 0.78 L seepage water after 13 cycles without noticeable efficiency decrease, revealing its exceptional stability and high efficiency with U-mine seepage water compared with the PC method. The U extraction capacity is calculated to be 0.48 gU $m^{-3}{\cdot}h^{-1}$ and 0.67 gU $m^{-3}{\cdot}h^{-1}$ at applied bias potentials of 0.5 V and 1.0 V, respectively, which are 12 – 17 times higher than the PC method. Moreover, the bias potential applied here served only as a driving force to separate the charge carriers (Figure S17). These results show that the PEC method has both higher U extraction efficiency and higher stability than the PC method in practical applications.

For the analysis of the feasibility of the proposed PEC U extraction method from the economic perspective, a cost-effective analysis is provided in Supplementary Note 11. We estimate that the cost for PEC U extraction from real U mine seepage water was $8.75/kgU and $15.63/kgU at 0.5 V and 1.0 V bias potential, respectively. In comparison, for the conventional terrestrial U resources, the acceptable exploitation cost is $260/kgU [47]. Hence, the extraction of

U from U mine tailings seepage water should be economically feasible.

On the global scale, a considerable amount of U is overlooked in over billions tons of mine tailings and is released into the environment via seepage water [2]. The present work successfully demonstrated the potential of the PEC method for U extraction from these seepage waters. For the U mine tailings where the studied seepage water was collected, the annual extractable U in the seepage water was 219 kg to 2190 kg, which accounts for up to 1.5‰ of the annual gross domestic U production of China [47]. Given the obtained U extraction capacity (0.48 ~ 0.67 gU $m^{-3}{\cdot}h^{-1}$) of the PEC method, this amount of U is fully recoverable if the PEC method is implemented. There are more than 908 million m^3 U mine tailings distributed in 163 U mining sites around the world [48], hence if the PEC method proposed herein can be applied to all of them, the annually extractable U could reach up to 10.7% of the annual global U consumption by the nuclear power industry (see Supplementary Note 12 for details). This can largely hedge the risks of the global U supply chain, as well as reduce the negative environmental impacts of U mining industry.

Other implications

Besides nuclear power, alternative renewable energies, *e.g.* wind, solar, and tidal energies, are also playing important roles in decarbonization. However, these non-nuclear alternative renewable energies are causing increasing load variability to the power grids due to their intermittent nature [49], so it is of vital importance to implement energy storage technology to mitigate such fluctuations. For long-term energy storage, converting and storing intermitting renewable electricity in the form of energy dense chemicals (*e.g.* H_2 gas, H_2O_2) is of particular interest to the energy sector [50]. On average, the net electrical energy density of U is estimated to be 43.3 MWh/kgU (Supplementary Note 13). In comparison, the gross energy densities of concentrated H_2O_2 (70% concentrated) and H_2 gas, the state-of-art energy storage chemicals, were 0.58 kWh/kg and 33.35 kWh/kg, respectively [50]. Hence, the net electrical power density of U is at least three and five orders of magnitude higher than the gross energy of H_2 gas and concentrated H_2O_2, respectively. Therefore, U is an ideal candidate for power-to-chemical energy storage. For the PEC U extraction method, the compulsory energy input is calculated to

be 70 ~ 125 kWh/kgU, without further optimization (Supplementary Note 11), which is only 0.16% ~ 0.29% of the energy density of the extracted U. This analysis implies that the PEC U extraction method has also great potential for energy storage applications.

Conclusions

In summary, we demonstrated the application of a PEC method to extract U from both synthetic U-containing water and mine tailings seepage water. The proposed PEC method can overcome the intrinsic drawbacks of the current photochemical methods by applying a bias potential on the photocatalyst, which drives spatial charge-carriers separation and decouples the U deposition sites and the photocatalyst active sites. As a result, the PEC method enables much faster U extraction and exceptional stability for both synthetic U-containing water and real U mine tailings seepage water. The economic analysis reveals that the proposed PEC U extraction method is an economically feasible approach. For the first time stable U(V) from aqueous media under ambient conditions was produced, implying the potential of the PEC method for the facile synthesis of U(V), which would facilitate future studies on U(V) chemistry. Further, the PEC U extraction method also exhibits high potential in energy storage applications. The present work is of interest to the nuclear power industry, uranium mining industry, geochemistry, and material chemistry.

Methods

Uranium extraction experiment

U extraction experiments were carried out using a single-compartment three-electrode reactor, which has an effective volume of 0.06 L. A 3 cm × 3 cm TiO_2 nanotube array (TNA) was used as the anode, as TiO_2 is the most developed and most commonly used model photocatalyst [51], and its conduction band edge potential is suitable for U(VI) reduction [13]. A 3 cm × 3.5 cm Ti foil was used as the cathode, because its capability of serving as the U deposition site has been demonstrated in previous extraction studies [15]. A saturated calomel electrode (SCE) was used as the reference electrode. An electrochemical workstation (CHI660E) was used to provide the designated bias on the TNA anode, and a UV-LED array with 60 mW/cm^2 irradiation was used as the light source. In the case of the PC method, the reactor was operated

at open-cell conditions without circuit connection between the TNA anode and the Ti electrode under illumination. In the case of the EC method, the system was operated in dark at designated bias potentials. Synthetic U-containing water was made by dissolving $UO_2(NO_3)_2 \cdot 6H_2O$ into ultra-pure water to reach desired concentrations. Meanwhile, 20 mM NaCl was also added as the supporting electrolyte, unless otherwise stated. For the real U-mine tailings seepage water experiments, seepage water collected from a decommissioned granite-related U mine tailings deposit was used after filtration by 0.2 μm filter membrane to remove suspended solids and microorganisms which may interfere the measurements. Detailed characterizations of the seepage water can be seen in Supplementary Note 10. Upon each cycle of the real U-mine tailings seepage water experiment, fresh Ti cathode was used while the TNA was continuously used without any means of regeneration. All experiments were conducted in the open-air. The U concentration was measured by a well-established spectrophotometric method as described in the literature [26]. The extracted mass of the U was calculated by comparing the difference between the remaining and the initial U concentration in the reaction solution.

Characterizations

Cyclic voltammetry (CV) characterizations of the Ti electrode were carried out using the CHI660E electrochemical workstation, with a 4 cm × 3 cm graphite plate as the counter electrode and a SCE reference electrode. Scanning electron microscopy (SEM) and energy dispersive spectroscopy (EDS) were conducted using a SU8010 ultra-high-resolution FE-SEM equipped with an X-Max N EDS system. X-ray photoelectron spectroscopy (XPS) was carried out using a Thermo K-Alpha+ XPS with an Al (Kα) source. X-ray diffraction (XRD) (Rigaku D-Mas 2500PC) was carried out using Cu Kα radiation.

References

1 Rhodes, R. More nuclear power can speed CO2 cuts. *Nature* **548**, 281-281, doi:10.1038/548281d (2017).

2 Dang, D. H., Wang, W., Pelletier, P., Poulain, A. J. & Evans, R. D. Uranium dispersion from U tailings and mechanisms leading to U accumulation in sediments: Insights from biogeochemical and isotopic approaches. *Science of The Total Environment* **610-611**, 880-891, doi:https://doi.org/10.1016/j.scitotenv.2017.08.156 (2018).

3 Bourrachot, S. *et al.* Effects of depleted uranium on the reproductive success and F1 generation survival of zebrafish (Danio rerio). *Aquatic Toxicology* **154**, 1-11, doi:https://doi.org/10.1016/j.aquatox.2014.04.018 (2014).

4 Zheng, M. *et al.* Efficient adsorption of europium (III) and uranium (VI) by titanate nanorings: Insights into radioactive metal species. *Environmental Science and Ecotechnology* **2**, 100031, doi:https://doi.org/10.1016/j.ese.2020.100031 (2020).

5 Yuan, Y. *et al.* Selective extraction of uranium from seawater with biofouling-resistant polymeric peptide. *Nature Sustainability*, doi:10.1038/s41893-021-00709-3 (2021).

6 Liu, C. *et al.* A half-wave rectified alternating current electrochemical method for uranium extraction from seawater. *Nature Energy* **2**, 17007, doi:10.1038/nenergy.2017.7 (2017).

7 Tsouris, C. Uranium extraction: Fuel from seawater. *Nature Energy* **2**, 17022, doi:10.1038/nenergy.2017.22 (2017).

8 Lively, D. S. S. R. P. Seven chemical separations to change the world. *Nature* **532**, 435–437 (2016).

9 Li, P. *et al.* An overview and recent progress in the heterogeneous photocatalytic reduction of U(VI). *Journal of Photochemistry and Photobiology C: Photochemistry Reviews* **41**, 100320, doi:https://doi.org/10.1016/j.jphotochemrev.2019.100320 (2019).

10 Liang, P.-l. *et al.* Photocatalytic reduction of uranium(VI) by magnetic ZnFe2O4 under visible light. *Applied Catalysis B: Environmental* **267**, 118688, doi:https://doi.org/10.1016/j.apcatb.2020.118688 (2020).

11 Deng, H. *et al.* Nanolayered Ti3C2 and SrTiO3 Composites for Photocatalytic Reduction and Removal of Uranium(VI). *ACS Applied Nano Materials* **2**, 2283-2294, doi:10.1021/acsanm.9b00205 (2019).

12 Lianos, P. Review of recent trends in photoelectrocatalytic conversion of solar energy to electricity and hydrogen. *Applied Catalysis B: Environmental* **210**, 235-254, doi:https://doi.org/10.1016/j.apcatb.2017.03.067 (2017).

13 Li, Z.-J. *et al.* Enhanced Photocatalytic Removal of Uranium(VI) from Aqueous Solution by Magnetic TiO2/Fe3O4 and Its Graphene Composite. *Environmental Science & Technology* **51**, 5666-5674, doi:10.1021/acs.est.6b05313 (2017).

14 Mazierski, P. *et al.* Removal of 5-fluorouracil by solar-driven photoelectrocatalytic oxidation using Ti/TiO2(NT) photoelectrodes. *Water Research* **157**, 610-620, doi:https://doi.org/10.1016/j.watres.2019.04.010 (2019).

15 Liu, T. *et al.* Removal and Recovery of Uranium from Groundwater Using Direct Electrochemical Reduction Method: Performance and Implications. *Environmental Science & Technology* **53**, 14612-14619, doi:10.1021/acs.est.9b06790 (2019).

16 Li, P. *et al.* Heterostructure of anatase-rutile aggregates boosting the photoreduction of U(VI). *Applied Surface Science* **483**, 670-676, doi:https://doi.org/10.1016/j.apsusc.2019.03.330 (2019).

17 Bonato, M., Ragnarsdottir, K. V. & Allen, G. C. Removal of Uranium(VI), Lead(II) at the Surface of TiO2 Nanotubes Studied by X-Ray Photoelectron Spectroscopy. *Water, Air, & Soil Pollution* **223**, 3845-3857, doi:10.1007/s11270-012-1153-1 (2012).

18 Li, H. *et al.* Revealing Principles for Design of Lean-Electrolyte Lithium Metal Anode via In Situ Spectroscopy. *Journal of the American Chemical Society* **142**, 2012-2022, doi:10.1021/jacs.9b11774 (2020).

19 Li, P. *et al.* Photoconversion of U(VI) by TiO2: An efficient strategy for seawater uranium extraction. *Chemical Engineering Journal* **365**, 231-241, doi:https://doi.org/10.1016/j.cej.2019.02.013 (2019).

20 Dlamini, T. C., Tshivhase, V. M., Maleka, P., Penabei, S. & Mashaba, M. The effect of

uranium speciation on the removal of gross alpha activity from acid mine drainage using anion exchange resin. *Journal of Radioanalytical and Nuclear Chemistry* **319**, 357-363, doi:10.1007/s10967-018-6354-7 (2019).

21 Garcia-Segura, S. & Brillas, E. Applied photoelectrocatalysis on the degradation of organic pollutants in wastewaters. *Journal of Photochemistry and Photobiology C: Photochemistry Reviews* **31**, 1-35, doi:https://doi.org/10.1016/j.jphotochemrev.2017.01.005 (2017).

22 Chen, J. *et al.* Tunneling Interlayer for Efficient Transport of Charges in Metal Oxide Electrodes. *Journal of the American Chemical Society* **138**, 3183-3189, doi:10.1021/jacs.5b13464 (2016).

23 Yuan, K. *et al.* Electrochemical and Spectroscopic Evidence on the One-Electron Reduction of U(VI) to U(V) on Magnetite. *Environmental Science & Technology* **49**, 6206-6213, doi:10.1021/acs.est.5b00025 (2015).

24 Gao, H. *et al.* CoS Quantum Dot Nanoclusters for High-Energy Potassium-Ion Batteries. *Advanced Functional Materials* **27**, 1702634, doi:https://doi.org/10.1002/adfm.201702634 (2017).

25 Li, D. *et al.* Foldable potassium-ion batteries enabled by free-standing and flexible SnS2@C nanofibers. *Energy & Environmental Science* **14**, 424-436, doi:10.1039/D0EE02919J (2021).

26 Kim, Y. K., Lee, S., Ryu, J. & Park, H. Solar conversion of seawater uranium (VI) using TiO2 electrodes. *Applied Catalysis B: Environmental* **163**, 584-590, doi:https://doi.org/10.1016/j.apcatb.2014.08.041 (2015).

27 Hennig, C., Ikeda-Ohno, A., Emmerling, F., Kraus, W. & Bernhard, G. Comparative investigation of the solution species U(CO3)56− and the crystal structure of Na6 U(CO3)5 · 12H2O. *Dalton Trans.* **39**, doi:10.1039/b922624a (2010).

28 Morris, D. E. Redox Energetics and Kinetics of Uranyl Coordination Complexes in Aqueous Solution. *Inorganic Chemistry* **41**, 3542-3547, doi:10.1021/ic0201708 (2002).

29 Janeczek, J. & Ewing, R. C. Structural formula of uraninite. *Journal of Nuclear Materials* **190**, 128-132, doi:https://doi.org/10.1016/0022-3115(92)90082-V (1992).

30 Eloirdi, R. *et al.* X-ray photoelectron spectroscopy study of the reduction and oxidation of uranium and cerium single oxide compared to (U-Ce) mixed oxide films. *Applied Surface Science* **457**, 566-571, doi:https://doi.org/10.1016/j.apsusc.2018.06.148 (2018).

31 Schindler, M., Hawthorne, F. C., Freund, M. S. & Burns, P. C. XPS spectra of uranyl minerals and synthetic uranyl compounds. I: The U 4f spectrum. *Geochimica et Cosmochimica Acta* **73**, 2471-2487, doi:https://doi.org/10.1016/j.gca.2008.10.042 (2009).

32 Butorin, S. M., Kvashnina, K. O., Prieur, D., Rivenet, M. & Martin, P. M. Characteristics of chemical bonding of pentavalent uranium in La-doped UO2. *Chemical Communications* **53**, 115-118, doi:10.1039/C6CC07684J (2017).

33 Gouder, T., Eloirdi, R. & Caciuffo, R. Direct observation of pure pentavalent uranium in U2O5 thin films by high resolution photoemission spectroscopy. *Scientific Reports* **8**, 8306, doi:10.1038/s41598-018-26594-z (2018).

34 El Jamal, G., Gouder, T., Eloirdi, R. & Jonsson, M. X-Ray and ultraviolet photoelectron spectroscopy studies of Uranium(iv),(v) and(vi) exposed to H2O-plasma under UHV conditions. *Dalton Transactions* **50**, 729-738, doi:10.1039/D0DT03562A (2021).

35 Belai, N., Frisch, M., Ilton, E. S., Ravel, B. & Cahill, C. L. Pentavalent Uranium Oxide via Reduction of [UO2]2+ Under Hydrothermal Reaction Conditions†. *Inorganic Chemistry* **47**, 10135-10140, doi:10.1021/ic801534m (2008).

36 Berthet, J.-C., Siffredi, G., Thuéry, P. & Ephritikhine, M. Easy access to stable pentavalent uranyl complexes. *Chemical Communications*, 3184-3186, doi:10.1039/B605710A (2006).

37 Graves, C. R. & Kiplinger, J. L. Pentavalent uranium chemistry—synthetic pursuit of a rare oxidation state. *Chemical Communications*, 3831-3853, doi:10.1039/B902969A (2009).

38 Yuan, K., Renock, D., Ewing, R. C. & Becker, U. Uranium reduction on magnetite:

Probing for pentavalent uranium using electrochemical methods. *Geochimica et Cosmochimica Acta* **156**, 194-206, doi:https://doi.org/10.1016/j.gca.2015.02.014 (2015).

39 Pan, Z. *et al.* Nanoscale mechanism of UO2 formation through uranium reduction by magnetite. *Nature Communications* **11**, 4001, doi:10.1038/s41467-020-17795-0 (2020).

40 Molinas, M. *et al.* Biological Reduction of a U(V)–Organic Ligand Complex. *Environmental Science & Technology*, doi:10.1021/acs.est.0c06633 (2021).

41 Chen, C.-S., Lee, S.-F. & Lii, K.-H. K(UO)Si2O6: A Pentavalent−Uranium Silicate. *Journal of the American Chemical Society* **127**, 12208-12209, doi:10.1021/ja0543853 (2005).

42 Zhang, M. *et al.* Intrinsic Semiconducting Behavior in a Large Mixed-Valent Uranium(V/VI) Cluster. *Angewandte Chemie International Edition* **n/a**, doi:https://doi.org/10.1002/anie.202017298.

43 Nocton, G., Horeglad, P., Pécaut, J. & Mazzanti, M. Polynuclear Cation−Cation Complexes of Pentavalent Uranyl: Relating Stability and Magnetic Properties to Structure. *Journal of the American Chemical Society* **130**, 16633-16645, doi:10.1021/ja804766r (2008).

44 Cui, W.-R. *et al.* Regenerable Covalent Organic Frameworks for Photo-enhanced Uranium Adsorption from Seawater. *Angewandte Chemie International Edition* **59**, 17684-17690, doi:https://doi.org/10.1002/anie.202007895 (2020).

45 Tondreau, A. M. *et al.* A Pseudotetrahedral Uranium(V) Complex. *Inorganic Chemistry* **57**, 8106-8115, doi:10.1021/acs.inorgchem.7b03139 (2018).

46 Arnold, P. L. *et al.* Strongly coupled binuclear uranium–oxo complexes from uranyl oxo rearrangement and reductive silylation. *Nature Chemistry* **4**, 221-227, doi:10.1038/nchem.1270 (2012).

47 NEA & IAEA. *Uranium 2020*. (2021).

48 IAEA. *The Long Term Stabilization of Uranium Mill Tailings*. (INTERNATIONAL ATOMIC ENERGY AGENCY, 2004).

49 Olauson, J. *et al.* Net load variability in Nordic countries with a highly or fully renewable power system. *Nature Energy* **1**, 16175, doi:10.1038/nenergy.2016.175 (2016).

50 Tang, J. *et al.* Selective hydrogen peroxide conversion tailored by surface, interface, and device engineering. *Joule* **5**, 1432-1461, doi:https://doi.org/10.1016/j.joule.2021.04.012 (2021).

51 Yang, H. G. *et al.* Anatase TiO2 single crystals with a large percentage of reactive facets. *Nature* **453**, 638-641, doi:10.1038/nature06964 (2008).

Acknowledgements

This work was supported by the National Natural Science Foundation of China (No. 42077352), the Key Research and Development Program of Shaanxi Province (2019KW-044) and the Fundamental Research Funds for the Central Universities (No. 31020200QD024, No. 3102019JC007).

Author Contributions

Y.Y. and Y.W. supervised the project. Y.Y. and Y.F. conceived the concept. Y.Y. and F.C. designed the experiments. J.J., Z.Q. and X.T. performed the experiments. Y.L. helped with the XRD characterization. M.L. and S.M. helped with the XPS and SEM characterizations. C.L., Y.L., Y.C., Y.F., F.C., Y.Y. and Y.W. analyzed the data. Y.Y., F.C., and Y.W. co-wrote the paper. All authors discussed and commented on the manuscript.

Competing Interests statement

The authors declare no competing financial interests.